

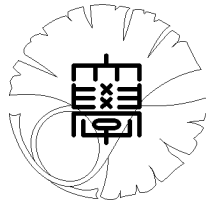
UTMS 2008–30

October 29, 2008

**Discretized Tikhonov regularization by a  
reproducing kernel Hilbert space for backward  
heat conduction problem**

by

Y. C. HON and Tomoya TAKEUCHI



**UNIVERSITY OF TOKYO**

GRADUATE SCHOOL OF MATHEMATICAL SCIENCES

KOMABA, TOKYO, JAPAN

# Discretized Tikhonov regularization by a reproducing kernel Hilbert space for backward heat conduction problem

Y. C. Hon\*and Tomoya Takeuchi†

## Abstract

In this paper we propose a numerical reconstruction method for solving a backward heat conduction problem. Based on the idea of reproducing kernel approximation, we reconstruct the unknown initial heat distribution from a finite set of scattered measurement of transient temperature at a fixed final time. Standard Tikhonov regularization technique using the norm of reproducing kernel is adopt to provide a stable solution when the measurement data contain noises. Numerical results indicate that the proposed method is stable, efficient, and accurate.

## 1 Introduction

Let  $\Omega \subset \mathbb{R}^d$ ,  $d \in \mathbb{N}$  be a bounded domain with sufficiently smooth boundary  $\partial\Omega$ . Consider the following initial boundary value problem for heat conduction equation:

$$\begin{cases} \partial_t u(t, x) = \Delta u(t, x), & x \in \Omega, t \in (0, t_f), \\ u(0, x) = f_0(x), & x \in \Omega; \\ u(t, x) = 0, & x \in \partial\Omega, t \in (0, t_f), \end{cases} \quad (1)$$

where  $t_f > 0$  is a fixed final time. The backward heat conduction problem (BHCP) is to recover the heat distribution at any earlier time  $0 \leq t < t_f$  from the temperature distribution  $u(t_f, \cdot)$ . This is a well known highly ill-posed problem [3, 25] in the Hadamard sense: There exists no solution in general that satisfies the heat equation with final data and the boundary conditions. Even if the solution exists, any small change in the observation data may induce enormous change in the solution. Moreover, in practical situation, the data  $u(t_f, \cdot)$  are collected only at a finite set of points  $\{z_1, \dots, z_M\} \subset \Omega$  and are contaminated with measurement noises. Therefore, most conventional numerical methods often fail to give an acceptable approximation to the solution of the BHCP.

There are quite a large number of works devoted to stable numerical methods for BHCP. The following is a partial list of articles which contain numerical tests: the method of fundamental solutions [22], boundary element method [10, 29], iterative boundary element method [21], inversion methods [18, 20],

---

\*Department of Mathematics, City University of Hong Kong, Hong Kong.

†Graduate School of Mathematical Sciences, University of Tokyo, Japan.

Tikhonov regularization by maximum entropy principle [23], operator-splitting methods [14], lattice-free finite difference method [12], Fourier regularization [7, 8], quasi-reversibility [15, 35], quasi-boundary regularization [4], modified methods [16, 26], group preserving scheme [17], regularization by semi-implicit finite difference method [30], nonlinear multigrid gradient method [36], approximate and analytic inversion formula [19]. Comparisons of some inverse methods can be found in [5, 24].

For stable reconstruction of the initial heat distribution, we employ a discretized Tikhonov regularization by the Ritz approach coupled with the reproducing kernel Hilbert space (RKHS), which is proposed in [31] and is applied to a Cauchy problem for an elliptic equation.

The outline of the paper is as follows: In section 2, we give a brief review on the results of the discretized Tikhonov regularization by reproducing kernel Hilbert space. The formulation of the BHCP problem is then given in section 3. In section 4 our reconstruction method for the solution is described for the BHCP. After the numerical implementation is mentioned in section 5, several numerical examples are given in section 6 to demonstrate the accuracy and efficiency of the proposed method.

## 2 The discretized Tikhonov regularization by Reproducing Kernel Hilbert Space

We begin with a brief review on the RKHS and the discretized Tikhonov regularization by RKHS. The general theory of Tikhonov regularization originates, for instance, from [32, 33]. The discretization of Tikhonov regularization by the Ritz approach can be found in [9]. As for the general theory of the reproducing kernel Hilbert space, one can refer to [1, 27].

**Definition 1.** Let  $\mathcal{H}$  be a real Hilbert space of functions defined on  $\Omega \subset \mathbb{R}^n$  with the inner product  $(\cdot, \cdot)_{\mathcal{H}}$ . A function  $\Phi: \Omega \times \Omega \rightarrow \mathbb{R}$  is called a *reproducing kernel* for  $\mathcal{H}$  if

1.  $\Phi(\cdot, x) \in \mathcal{H}$  for all  $x \in \Omega$ ,
2.  $f(x) = (f, \Phi(\cdot, x))_{\mathcal{H}}$  for all  $f \in \mathcal{H}$  and all  $x \in \Omega$ .

We define the norm by  $\|f\|_{\mathcal{H}} = (f, f)_{\mathcal{H}}^{\frac{1}{2}}$ .

A Hilbert space of functions which admits a reproducing kernel is called a *reproducing kernel Hilbert space* (in short, RKHS). The reproducing kernel of a RKHS is uniquely determined. Conversely, if  $\Phi$  is a symmetric positive definite kernel, then one can construct a unique RKHS in which the given kernel acts as the reproducing kernel (see [34] for details).

For later convenience, we list in the following some fundamental properties of RKHS:

1.  $\Phi(x, y) = (\Phi(\cdot, x), \Phi(\cdot, y))_{\mathcal{H}}$  for all  $x, y \in \Omega$ .
2.  $\|f\|_{\mathcal{H}}^2 = \sum_{k=1}^N \sum_{j=1}^N \alpha_k \alpha_j \Phi(x_k, x_j)$ , for all  $f \in \mathcal{H}$  in the form of  $f = \sum_{k=1}^N \alpha_k \Phi(\cdot, x_k)$  with  $x_k \in \Omega$ .

3. Let  $T_\Phi(v)(x) = \int_\Omega \Phi(x, y)v(y)dy$ ,  $v \in L^2(\Omega)$ ,  $x \in \Omega$ . From Mercer's theorem  $\Phi$  can be represented as

$$\Phi(x, y) = \sum_{j=1}^{\infty} \lambda_j \varphi_j(x) \varphi_j(y),$$

where  $\lambda_j$  are the non-negative eigenvalues and  $\varphi_j$  are the eigenfunctions of  $T_\Phi$ .

4.  $\mathcal{H}$  is given by

$$\mathcal{H} = \left\{ f \in L^2(\Omega) \mid \sum_{j=1}^{\infty} \lambda_j^{-1} |(f, \varphi_j)_{L^2(\Omega)}|^2 < \infty \right\},$$

and the inner product can be written as

$$(f, g)_\mathcal{H} = \sum_{j=1}^{\infty} \lambda_j^{-1} (f, \varphi_j)_{L^2(\Omega)} (g, \varphi_j)_{L^2(\Omega)}, \quad f, g \in \mathcal{H}.$$

Now, we briefly describe the discretized Tikhonov regularization by RKHS. For a finite set of points  $X_m := \{x_1, \dots, x_m\} \subset \Omega$  and  $f \in \mathcal{H}$ , we consider the finite sum  $s_{f, X_m}(x) = \sum_{k=1}^m \alpha_k \Phi(x, x_k)$ , where the coefficients  $\{\alpha_k\}_{k=1}^m$  are determined uniquely by the system  $s_{f, X_m}(x_k) = f(x_k)$ ,  $1 \leq k \leq m$ , since  $\Phi$  is positive definite.

Define a subspace  $V_m$ ,  $V_m := \text{span} \{\Phi(\cdot, x) \mid x \in X_m\} \subset \mathcal{H}$  and an operator  $P_m: \mathcal{H} \rightarrow V_m \subset \mathcal{H}$  by  $P_m(f)(x) = s_{f, X_m}(x)$ .

Let  $W$  be any Hilbert space and  $K$  be a linear compact operator from  $\mathcal{H}$  to  $W$ . We consider the reconstruction of  $f_0 \in \mathcal{H}$  in the following equation

$$K f_0 = g_0 \tag{2}$$

from noisy data  $g_\delta$  with  $\|g_0 - g_\delta\|_W \leq \delta$ . In order to stably reconstruct  $f_0$  from noisy data  $g_\delta$ , we consider the discretized Tikhonov regularization:

$$\min_{f \in V_m} \|K f - g_\delta\|_W^2 + \alpha \|f\|_\mathcal{H}^2 \tag{3}$$

It is well known that the solution of the minimization problem can be uniquely determined [2] and we denote the minimizer by  $f_{\alpha, m, \delta}$ . We can establish the convergence of  $f_{\alpha, m, \delta}$  to the minimum norm solution  $K^\dagger g_0$  of  $K f_0 = g_0$  if we choose  $m = m(\delta)$  and  $\alpha = \alpha(\delta)$  suitably with respect to the noise level  $\delta$ . To state the convergence result, we fix the notations and introduce some assumptions.

Let us define the fill distance  $h_m$  of  $X_m$  by  $h_m = \sup_{x \in \Omega} \min_{x_j \in X_m} \|x - x_j\|$ . We choose the finite set of points  $X_m$  such that  $\lim_{m \rightarrow \infty} h_m = 0$ . Let  $\gamma_m := \|K(I - P_m)\|$ , here  $I: \mathcal{H} \rightarrow \mathcal{H}$  is the identity map. Let  $\lim_{\delta \rightarrow 0} m(\delta) = \infty$  and  $\lim_{\delta \rightarrow 0} \alpha(\delta) = 0$ . The next theorem shows that the solution  $f_{\alpha, m, \delta}$  of (3) converges to the minimum norm solution  $K^\dagger g_0$  of (2).

**Theorem 2.** Assume that the kernel  $\Phi$  is uniformly continuous on  $\Omega \times \Omega$  and  $\lim_{m \rightarrow \infty} \gamma_m = 0$ . If  $\gamma_m = O(\sqrt{\alpha})$  and  $\delta = O(\sqrt{\alpha})$ , then  $\lim_{\delta \rightarrow 0} \|f_{\alpha(\delta), m(\delta), \delta} - K^\dagger g_0\|_{L^2(\Omega)} = 0$ .

For the noise-free data case, we have

**Theorem 3.** Let  $\lim_{m \rightarrow \infty} \alpha_m = 0$ . If  $\gamma_m = O(\sqrt{\alpha_m})$ , then  $\lim_{m \rightarrow \infty} \|f_{\alpha_m, m} - K^\dagger g_0\|_{L^\infty(\Omega)} = 0$ .

For the detail description of the discretized Tikhonov regularization by RKHS including the proof of the theorem can be found in [31].

The above result is valid independent of the choice of any reproducing kernel  $\Phi$  satisfying the assumption in Theorem 2, and one can use any kernel for a numerical reconstruction at least in principle. Taking into account that the solution satisfies the Dirichlet boundary condition and the fact that our approximate solution is constructed in the form of the finite sum of the kernel, the kernel should satisfy the boundary condition as well. One possible choice for the kernel is the Green's function of the heat equation (8) and we show that the Green's function satisfies the assumption in Theorem 2 in section 4.

### 3 Formulation of the Inverse problem

We now formulate our inverse problem. The inverse problem to be investigated in this paper is to reconstruct the unknown initial heat distribution  $f_0$  of (8) from some scattered noisy data  $u_\delta(t_f, z_j) = u(t_f, z_j) + noise$ .

Let  $\Phi: \Omega \times \Omega \rightarrow \mathbb{R}$  be a positive definite kernel and let  $\mathcal{H}$  be the RKHS generated by the kernel  $\Phi$  which is uniformly continuous on  $\Omega \times \Omega$ . Let us assume that the initial value  $u(0, x)$  belongs to the space  $\mathcal{H}$ .

The unique solution of the equation (8) with initial value  $u(0, x) = f \in \mathcal{H}$  can be written as

$$u(t, x) = \int_{\Omega} f(y)G(t, x, y)dy,$$

where  $G(t, x, y)$  is the Green's function satisfying Dirichlet condition [13]. For each  $f \in \mathcal{H}$  we define a map  $K_0: \mathcal{H} \rightarrow L^2(\Omega)$  as

$$K_0 f(x) := \int_{\Omega} f(y)G(t_f, x, y)dy.$$

Let  $K: \mathcal{H} \rightarrow \mathbb{R}^M$  be defined by  $Kf := (K_0 f(z_1), \dots, K_0 f(z_M)) \in \mathbb{R}^M$  and let  $u_{t_f} := (u(t_f, z_1), \dots, u(t_f, z_M)) \in \mathbb{R}^M$ . The inverse problem in (1) is stated as follows:

Find the minimum norm solution  $K^\dagger u_{t_f} \in \mathcal{H}$  of the system

$$K f_0 = u_{t_f}$$

from a scattered noisy data  $u_{t_f}^\delta = (u_\delta(z_1), \dots, u_\delta(z_M)) \in \mathbb{R}^M$  observed at points  $Z = \{z_1, \dots, z_M\} \subset \Omega$  and at a fixed final time  $t_f > 0$  with prescribed error bound  $\delta$ :

$$\sum_{k=1}^M |u_\delta(z_k) - u(t_f, z_k)|^2 \leq \delta^2.$$

## 4 The reconstruction of the initial heat distribution

We adapt the discretized Tikhonov regularization by using RKHS for stable reconstruction  $K^\dagger u_{t_f}$  from the noisy data  $u_{t_f}^\delta \in \mathbb{R}^M$ :

$$\min_{f \in V_m} \|Kf - u_{t_f}^\delta\|_{\mathbb{R}^M}^2 + \alpha \|f\|_{\mathcal{H}}^2, \quad (4)$$

where  $\alpha > 0$  is called a regularizing parameter.

As we mention above, the kernel may in principle be chosen arbitrary if it satisfies the condition in Theorem 2. However, we focus ourselves on the special kernel that automatically satisfies the Dirichlet boundary condition for accurate reconstruction, namely, the Green's function of the heat equation (8). It is not obvious if the Green's function satisfies the condition.

Let us begin with the following Lemma.

**Lemma 1.** *Let  $t_f > t_0 > 0$  be given. Define  $\Phi(x, y) := G(t_0, x, y)$ . Then  $\Phi: \Omega \times \Omega \rightarrow \mathbb{R}$  is symmetric and positive definite.*

*Proof.* We just need to show that

$$\sum_{j=1}^n \sum_{k=1}^n \alpha_j \alpha_k G(t_0, x_j, x_k) > 0$$

for all  $n \in \mathbb{N}$ , all pairwise distinct points  $\{x_1, \dots, x_n\} \subset \Omega$  and for all  $(\alpha_1, \dots, \alpha_n) \in \mathbb{R}^n \setminus \{0\}$ .

The following two properties of the Green's function

$$\int_{\Omega} G(t, x, z) G(s, z, y) dz = G(t + s, x, y), \quad \text{for all } s, t > 0,$$

and

$$G(t, x, y) = G(t, y, x) \quad \text{for all } t > 0, x, y \in \overline{\Omega},$$

yield

$$\begin{aligned} \sum_{j=1}^n \sum_{k=1}^n \alpha_j \alpha_k G(t_0, x_j, x_k) &= \sum_{j=1}^n \sum_{k=1}^n \alpha_j \alpha_k \int_{\Omega} G\left(\frac{t_0}{2}, x_j, y\right) G\left(\frac{t_0}{2}, y, x_k\right) dy \\ &= \int_{\Omega} \left( \sum_{j=1}^n \alpha_j G\left(\frac{t_0}{2}, x_j, y\right) \right)^2 dy =: I \geq 0. \end{aligned}$$

The lemma will be verified if  $I \neq 0$ . Consider the following heat equation

$$\begin{cases} \partial_t u(t, x) = \Delta u(t, x), & x \in \Omega, t > 0, \\ u(t, x) = 0, & x \in \partial\Omega, t > 0, \\ u(0, x) = \sum_{k=1}^n \alpha_k \delta(x - x_k), & x \in \Omega. \end{cases}$$

where  $\delta(x - x_k)$  is the dirac measure with center located at  $x_k$  whose unique solution is written in terms of the Green's function  $G(t, x, y)$  as

$$u(t, x) = \sum_{k=1}^n \alpha_k G(t, x_k, x), \quad \text{for } t > 0.$$

If  $I = 0$ , we then have  $u(t_0/2, x_k, x) = 0$  for all  $x \in \bar{\Omega}$ . Therefore we have  $u(t, x_k, x) = 0$  for all  $x \in \bar{\Omega}$  and for all  $0 < t < t_0/2$ . As a result, we have that  $\sum_{k=1}^n \alpha_k \delta(x - x_k) = 0$  in the distribution sense, which implies that  $\alpha_k = 0$  for all  $k = 1, \dots, n$ . This contradicts to  $\alpha \in \mathbb{R}^n \setminus \{0\}$ .  $\square$

Henceforth we denote by  $\mathcal{H}_{t_0}$  the RKHS generated by the kernel  $G(t_0, x, y)$ . Since the Green's function  $G(t, x, y)$  is expanded in the eigenfunctions  $\varphi_k$  and non-negative eigenvalues  $\lambda_j$  of Laplace operator  $\Delta$  with Dirichlet boundary condition as  $G(t, x, y) = \sum_{j=1}^{\infty} e^{-\lambda_j t} \varphi_j(x) \varphi_j(y)$  (see [6]), the space  $\mathcal{H}_{t_0}$  is given by

$$\mathcal{H}_{t_0} = \left\{ f \in L^2(\Omega) \mid \sum_{j=1}^{\infty} e^{\lambda_j t_0} |(f, \varphi_j)_{L^2(\Omega)}|^2 < \infty \right\}.$$

Next we show the two conditions in Theorem 2, that is, (1)  $\Phi$  is uniformly continuous on  $\Omega$  and (2)  $\gamma_m = \|K(I - P_m)\| \rightarrow 0$  as  $m \rightarrow \infty$ . The former condition is satisfied because the Green's function  $G(t_0, x, y)$  is smooth on  $\bar{\Omega} \times \bar{\Omega}$  [6]. We shall check that (2) is satisfied.

**Lemma 2.**  $\gamma_m = \|K(I - P_m)\| \rightarrow 0$  as  $m \rightarrow \infty$ .

*Proof.* Since, for a fixed  $t_0 > 0$  and for any  $y \in \Omega$ , the function  $G(t_0, x, y)$  is smooth, the RKHS  $\mathcal{H}$  generated by the kernel  $\Phi(x, y) = G(t_0, x, y)$  is continuously embedded in a Sobolev space  $W_2^m(\Omega)$  with sufficiently large  $m > 0$ . With the help of Sobolev norm estimates for functions which vanish on a finite set of points in a domain  $\Omega$ , we can find a function  $p: \mathbb{R}_+ \rightarrow \mathbb{R}_+$  satisfying  $\lim_{r \rightarrow 0} p(r) = 0$  such that the estimate

$$\|f - P_m f\|_{L^\infty(\Omega)} \leq p(h_{X_m}) \|f\|_{\mathcal{H}} \quad (5)$$

holds for all  $f \in \mathcal{H}$ . Therefore we assume that the existence such function  $p$ . The above discussion is based on the section 5 in [28]. For the detail treatise of the estimate one can refer [34] and the references therein.

Since  $\|G(t_f, x, \cdot)\|_{L^1(\Omega)} = 1$  for  $x \in \Omega$ ,

$$\begin{aligned} \|Kf\|_{\mathbb{R}^M} &\leq \max_{1 \leq k \leq M} |K_0 f(x_k)| = \max_{1 \leq k \leq M} \left| \int_{\Omega} G(t_f, x_k, z) f(z) dz \right| \\ &\leq M \|f\|_{L^\infty(\Omega)} \end{aligned}$$

for all  $f \in \mathcal{H}$ . By the property of RKHS,  $\|f\|_{L^\infty(\Omega)} \leq \sup_{x \in \Omega} \sqrt{\Phi(x, x)} \|f\|_{\mathcal{H}}$ . Thus, we have

$$\|K(I - P_m)f\|_{\mathbb{R}^M} \leq M \|(I - P_m)f\|_{L^\infty(\Omega)} \leq Mp(h_m) \|f\|_{\mathcal{H}}.$$

The last inequality follows from (5). Hence,

$$\lim_{m \rightarrow \infty} \|K(I - P_m)\| = \lim_{m \rightarrow \infty} \sup_{f \in \mathcal{H}} \frac{\|K(I - P_m)f\|_{\mathbb{R}^M}}{\|f\|_{\mathcal{H}}} \leq \lim_{m \rightarrow \infty} Mp(h_m) = 0.$$

$\square$

Thus, it follows that the unique solution of (4) converges to the minimum norm solution  $K^\dagger u_{t_f}$ . We then have

**Theorem 4.** *If  $\gamma_m = O(\sqrt{\alpha})$  and  $\delta = O(\sqrt{\alpha})$ , then  $\lim_{\delta \rightarrow 0} \|f_{\alpha(\delta), m(\delta), \delta} - K^\dagger u_{t_f}\|_{L^2(\Omega)} = 0$ .*

For the noise-free data case, we have

**Theorem 5.** *Let  $\lim_{m \rightarrow \infty} \alpha_m = 0$ . If  $\gamma_m = O(\sqrt{\alpha_m})$ , then  $\lim_{m \rightarrow \infty} \|f_{\alpha_m, m} - K^\dagger u_{t_f}\|_{L^\infty(\Omega)} = 0$ .*

## 5 Numerical implementation

$V_m$  is spanned by the finite sum of  $G(t_0, \cdot, x_k)$  with  $x_k \in X_m \subset \Omega$ , and therefore the minimizer  $f_{\alpha, m, \delta}$  is written as

$$f_{\alpha, m, \delta} = \sum_{k=1}^m \lambda_k G(t_0, \cdot, x_k), \quad x_k \in X_m.$$

Note that the minimizer so constructed automatically satisfies the Dirichlet boundary condition, *i.e.*,  $f_{\alpha, m, \delta}|_{\partial\Omega} = 0$ .

**Lemma 3.** *The coefficients  $\lambda_{\min} = \{\lambda_k\}_{k=1}^m \in \mathbb{R}^m$  is the unique solution of the system*

$$(A^* A + \alpha B) \lambda_{\min} = A^* u_{t_f}^\delta, \quad (6)$$

where  $u_{t_f}^\delta = (u_\delta(z_1), \dots, u_\delta(z_M))^\top \in \mathbb{R}^M$ ,  $A$  is a  $M \times m$  matrix and  $B$  is a  $m \times m$  matrix defined by

$$\begin{cases} A_{j,k} = G(t_0 + t_f, z_k, x_j), & j = 1, \dots, M, \quad k = 1, \dots, m, \\ B_{j,k} = G(t_0, x_j, x_k), & j, k = 1, \dots, m. \end{cases}$$

Here,  $A^*$  denotes the transpose of the matrix  $A$ .

*Proof.* From the definition of RKHS [34], it follows that  $\|f\|_{\mathcal{H}}^2 = \sum_{i,j=1}^m \lambda_i \lambda_j G(t_0, x_i, x_j)$

for  $f \in V_m$  and some  $\lambda_k \in \mathbb{R}$ ,  $k = 1, \dots, m$ . Since  $KG(t_0, \cdot, x_k) = \int_{\Omega} G(t_0, y, x_k) G(t_f, \cdot, y) dy = G(t_0 + t_f, \cdot, x_k)$ , the minimization problem is equivalent to the following minimization problem:

$$\min_{\lambda \in \mathbb{R}^m} \left\| \sum_{k=1}^m \lambda_k G(t_0 + t_f, \cdot, x_k) - u_{t_f}^\delta \right\|_{\mathbb{R}^M}^2 + \alpha \sum_{i=1}^m \sum_{j=1}^m \lambda_i \lambda_j G(t_0, x_i, x_j).$$

Now, it is easy to see that the coefficients  $\lambda_{\min} \in \mathbb{R}^m$  satisfies the equation (6).  $\square$

## 6 Numerical experiments

### 6.1 Noise-free data

In this section we verify the numerical efficiency and accuracy of the proposed reconstruction method. For the purpose of comparison with existing works,[4, 15, 20, 21, 22], the numerical experiments are conducted with the following typical bench-mark test problem:

**Example 1** We consider the one-dimensional BHCP

$$\begin{cases} \partial_t u(t, x) = \Delta u(t, x), & x \in (0, 1), t \in (0, t_f), \\ u(0, x) = \sin(\pi x), & x \in (0, 1); \\ u(t, 0) = u(t, 1) = 0, & t \in (0, t_f), \end{cases} \quad (7)$$

whose exact solution is given by  $u(t, x) = \sin(\pi x) \exp(\pi^2 t)$ . We reconstruct numerically the initial temperature distribution  $\sin(\pi x)$  from the knowledge of the final time temperature distribution  $u(t_f, x)$ .

The Green's function  $G(t, x, y)$  is given as  $G(t, x, y) = \sum_{j=1}^{\infty} e^{-j^2 \pi^2 t} \sin(j \pi x) \sin(j \pi y)$

and the space  $\mathcal{H}_{t_0}$  is given by

$$\mathcal{H}_{t_0} = \left\{ f \in L^2(\Omega) \mid \sum_{j=1}^{\infty} e^{j^2 \pi^2 t_0} |(f, \sin(j \pi x))_{L^2(\Omega)}|^2 < \infty \right\}.$$

It is easy to see that the initial condition  $u(0, x) = \sin \pi x$  belongs to the space  $\mathcal{H}_{t_0}$  for any  $t_0$ .

To obtain a numerical solution with our method, we have to determine  $t_0$ ,  $X_m$ , measurement points  $Z_M := \{z_k\}_M$  and observation time  $t_f$  to define  $A$ ,  $B$  and the data  $\{u(t_f, z_k)\}_{k=1}^M$ . Then, we solve the equation (6) with suitable parameter  $\alpha$ .

The matrices  $A$  and  $B$  depend on various quantities, i.e.,  $A = A(t_0, t_f, X_m, Z_M)$  and  $B = B(t_0, X_m)$ . However, we omit such dependence. Firstly, we employ our method with the case  $t_f = 1.5, 2.5, 3$  to compare the accuracy of our results with those obtained by [4]. These problems are highly ill-posed. We must recover the initial data with the order of  $O(1)$  from the final data with the order of  $O(10^{-7}) - O(10^{-13})$ .

According to the convergence theorem for noise free data case, larger  $m$  in  $X_m$  will yield better numerical solution. Due to the ill-posedness of BHCP, the matrix  $A^*A$  is ill-conditioned. As a result, the numerical computation of the inverse of  $A^*A + \alpha B$  is impossible when the regularizing term  $B$  is also ill-conditioned. To see the effect of increasing number of  $m$  to the condition number of  $B$ ,  $\text{cond}(B)$ , of the matrix  $B = \{G(t_0, x_i, x_j)\}_{i,j}$ , we plot  $\text{cond}(B)$  verse the number of  $m$  running from 10 to 200. In this test,  $X_m$  is chosen as  $X_m = \left\{ \frac{1}{m+1}, \dots, \frac{m}{m+1} \right\}$  for each  $m$ . We show the results for the cases  $t_0 = 10^{-2}$ ,  $t_0 = 10^{-3}$  and  $t_0 = 10^{-4}$  in Figure 1. In all cases,  $\text{cond}(B)$  increase exponentially as  $m$  increase which means the matrix  $B$  corresponding larger  $m$  may not work as the regularization.

Next, we show the effect of the increasing number of  $m$  to the accuracy of our numerical solution for each  $t_0 = \{10^{-2}, 10^{-3}, 10^{-4}\}$ .  $X_m$  is given in the

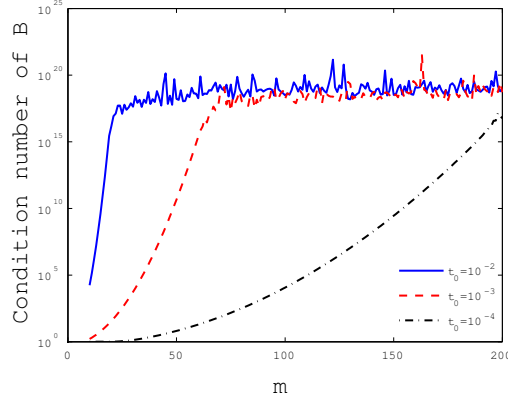


Figure 1: The effect of the increasing number of  $m$  to the condition number of  $B$  for the case  $t_0 \in \{10^{-2}, 10^{-3}, 10^{-4}\}$ .

same way as above. We give 30 measurement points  $Z_{30} = \{\frac{k}{30+1} \mid k = 1, \dots, 30\}$  and use the measurement data for the case  $t_f = 3$ . We solve the system  $(A^*A + \alpha B)\lambda_{\min} = A^*u_{t_f}$ ,  $u_{t_f} = [u(t_f, z_1), \dots, u(t_f, z_{30})]^T$  to obtain  $\lambda$  in

$$f_{\alpha, m}(x) = \sum_{k=1}^m \lambda_k G(t_0, x_k, x).$$

Although we should select  $\alpha$  depending on  $m$  so that  $\gamma_m = O(\sqrt{\alpha m})$  as in Theorem 5, we pick  $\alpha$  as  $\alpha = 10^{-5} \frac{\max(A^*A)}{\max(B)}$ , where  $\max(C) = \max_{i,j} c_{i,j}$  for a matrix  $C = (c_{i,j})$ . To avoid numerical instability when calculating the inverse of  $A^*A + \alpha B$ , we restrict the range of the number  $m$  such that  $\text{cond}(B) < 10^{17}$  for each  $t_0$ . That is,  $m = 10$  to 21 for  $t_0 = 10^{-2}$ ,  $m = 10$  to 65 for  $t_0 = 10^{-3}$  and  $m = 10$  to 197 for  $t_0 = 10^{-4}$ . The maximum error  $E(m) = \|f_{\alpha, m} - u(0, \cdot)\|_{L^\infty(0,1)}$  for each  $t_0$  are reported in Figure 2, which shows that the accuracy in the numerical solution decreases as  $m$  increases. However, for the case  $t_0 = 10^{-4}$ , the accuracy begins to increase after  $m = 140$ .

At the end, we show the numerical results for the cases  $t_f = \{1.5, 2.5, 3\}$  under the setting,  $M = 30$ ,  $t_0 = 10^{-4}$  and  $m = 120$ . Figure 3 shows the absolute error for these three cases. Each of the maximum error occurs at  $x = 0.5$  and they are  $7.1 \times 10^{-7}$  for  $t_f = 1.5$ ,  $1.3 \times 10^{-6}$  for  $t_f = 2.5$ , and  $4.8 \times 10^{-4}$  for  $t_f = 3$ , respectively. We omit these plots here because the numerical results are so accurate as shown in Figure 3 that the graph of these results almost coincide with the exact solution  $u(0, x) = \sin \pi x$  and we cannot see the difference between them. For comparison, we cite the maximum error reported in [4] which is about  $2.8 \times 10^{-3}$  for the case of  $t_f = 3$ .

**Example 2** We test the performance of our method by using the following example which is a hard benchmark problem of BHCP. We consider the one-

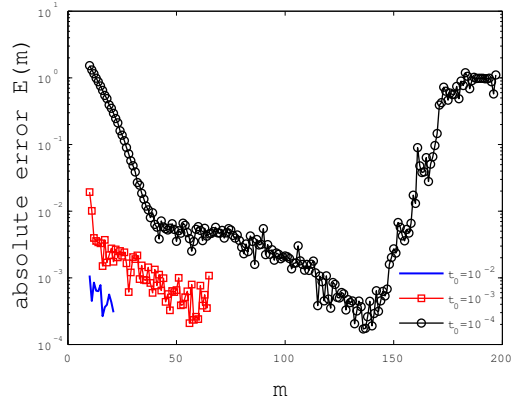


Figure 2: The effect of the increasing number of  $m$  to the accuracy of the numerical solution with various  $t_0 = \{10^{-2}, 10^{-3}, 10^{-4}\}$  for the case of  $t_f = 3$  and  $M = 30$ .

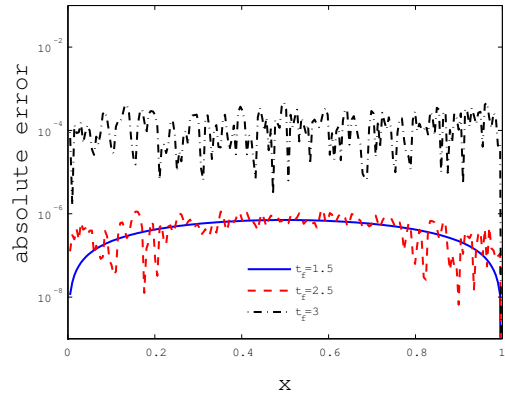
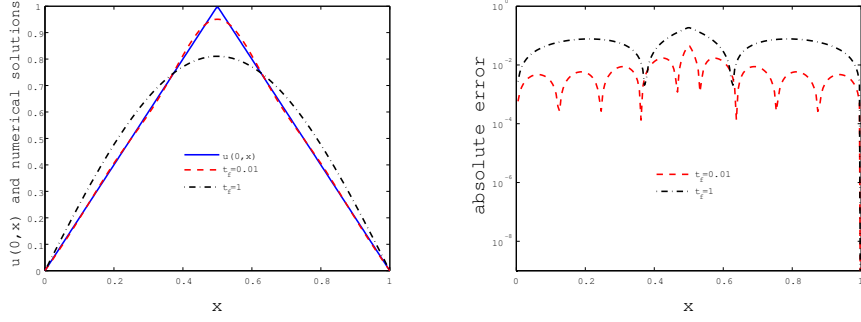


Figure 3: The numerical errors for the case  $t_f = \{1.5, 2.5, 3\}$ . The numerical solution is obtained under the condition  $t_0 = 10^{-4}$ ,  $m = 120$  and  $M = 30$ .



(a)  $u(0, x) = 2 \min(x, 1 - x)$  and numerical solutions (b) Absolute error in the numerical solutions

Figure 4: Exact solution  $u(0, x) = 2 \min(x, 1 - x)$  and numerical solutions for  $t_f = 0.01$  and  $t_f = 1$ . The other parameters are set as  $t_0 = 10^{-4}$ ,  $m = 120$  and  $M = 30$ .

dimensional BHCP

$$\begin{cases} \partial_t u(t, x) = \Delta u(t, x), & x \in (0, 1), t \in (0, t_f), \\ u(0, x) = 2 \min(x, 1 - x), & x \in (0, 1); \\ u(t, 0) = u(t, 1) = 0, & t \in (0, t_f), \end{cases} \quad (8)$$

The exact solution is given by

$$u(t, x) = \sum_{k=1}^{\infty} \frac{8(-1)^{k+1}}{(2k-1)^2 \pi^2} \sin\{(2k-1)\pi x\} \exp(-(2k-1)^2 \pi^2 t).$$

We construct numerically the initial temperature distribution  $2 \min(x, 1 - x)$  from the knowledge of the final time temperature distribution  $u(t_f, x)$ . Note that the function  $2 \min(x, 1 - x)$  is not smooth at  $x = 0.5$  and hence it does not belong to the solution space  $\mathcal{H}_{t_0}$  for any  $t_0 > 0$ . Therefore, our theory does not guarantee that we can recover this initial condition. We report the numerical results for the cases  $t_f = \{0.01, 1\}$  obtained under the setting  $M = 30$ ,  $t_0 = 10^{-4}$  and  $m = 120$ . The exact solution  $u(0, x)$  and the numerical solutions are graphically shown in Figure 4(a). In Figure 4(b) the absolute errors  $|u(0, x) - f_{\alpha, m}(x)|$  for both cases are reported. The maximum errors are  $4.4 \times 10^{-2}$  for  $t_f = 0.01$  and  $1.8 \times 10^{-1}$  for  $t_f = 1$ , respectively. Even for this severe problem, our method is capable of giving the satisfactory results.

## 6.2 Noisy data

We verify the numerical accuracy of the proposed method for the case when the data contains noise by using Example 1. We fix  $t_f = 0.25$  and  $M = 30$  throughout of this section. The noisy data  $u_{0.25}^{\delta}$  at measurement points  $Z_{30} = \{z_j \mid z_j = \frac{j}{30+1}\}$  are obtained by adding random numbers to the exact data  $u(0.25, x)$  by

$$u_{0.25}^{\delta}(z_j) = u(0.25, z_j) + \frac{\delta}{100} \max_{z_j \in Z_{30}} |u(0.25, z_j)| \text{rand}(j)$$

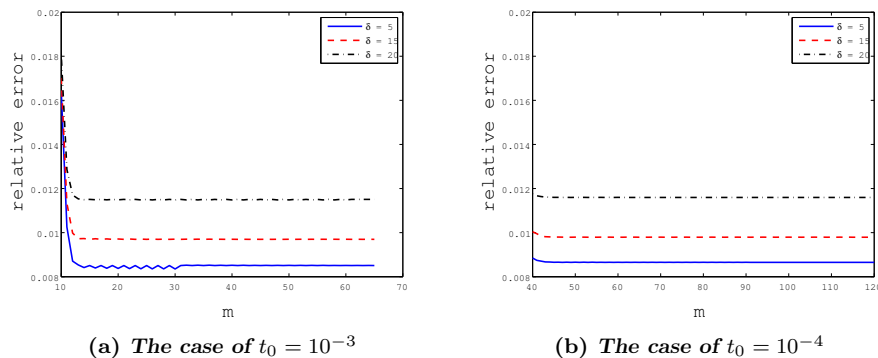


Figure 5: Relative error of the reconstructed numerical solution  $U$ . The final time  $t_f = 0.25$ ,  $t_0 = 10^{-3}$  and  $M = 30$ .

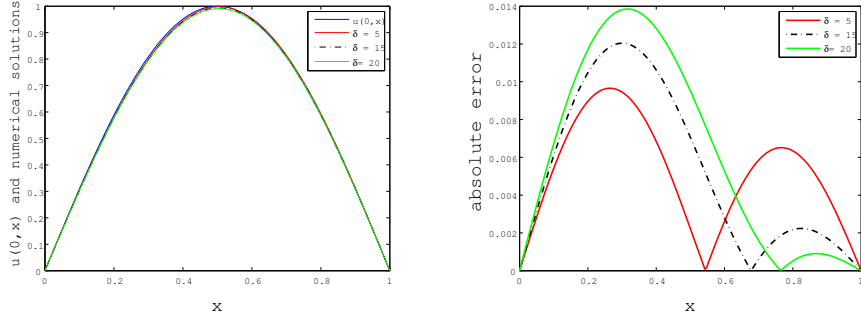
for  $j = 1, \dots, 30$ , where  $u(0.25, z_j)$  is the exact data in (8) and  $\text{rand}(j)$  is a random number between  $[-1, 1]$  and  $\delta\% \in \{5\%, 15\%, 20\%\}$  is noise level. For all given noisy data  $u_{0.25}^\delta$  with various noisy data, we apply the proposed method to obtain an approximate solution to  $u(0, x)$ . We denote the reconstructed numerical solution by  $U$ .

The regularization parameter  $\alpha$  has to be chosen appropriately according to the noise level prescribed in Theorem 4. However, in practice the noise level may not always be given and hence it is necessary to consider also error-free parameter choice rules that compensate this lack of information for the noise level. Here, the L-curve criterion [11] is adopted for choosing the regularization parameter.

At first, we study the effect of the number  $m$  to the accuracy of the numerical solution  $U$  with various noisy level and various  $t_0$ . For the numerical error estimations, we compute the relative error of the reconstructed solutions which we denote by  $R(U)$ :

$$R(U) = \frac{\|U - u(0, \cdot)\|_{L^2(0,1)}}{\|u(0, \cdot)\|_{L^2(0,1)}}.$$

Figure 5(a) plots the relative error  $R(U)$  for each  $m$  for the case of  $t_0 = 10^{-3}$ . The number  $m$  runs from 10 to 65. It can be seen from Figure 5(a) that large  $m$  does not affect the accuracy of  $U$ . The result for the case of  $t_0 = 10^{-4}$  is reported in Figure 5(b) where  $m$  runs from 40 to 120. We can see the same trend as that for the case of  $t_0 = 10^{-3}$ . We can conclude that  $t_0$  and the number  $m$  do not affect the accuracy of the numerical solution if  $m$  is not too small, and our method still gives reasonable approximations to the solution  $u(0, x)$ . At the end of this section, we show some numerical results with various noise level  $\delta\% \in \{5\%, 15\%, 20\%\}$ . The parameters are  $t_0 = 10^{-3}$ ,  $m = 30$ ,  $t_f = 0.25$  and  $M = 30$ . The exact solution  $u(0, x) = \sin \pi x$  and the numerical solutions are shown in Figure 6(a) and the absolute error in Figure 6(b). It can be observed that the method works for the case of Example 2 with noisy data as well.



(a)  $u(0, x) = \sin \pi x$  and numerical solutions (b) Absolute error in the numerical solutions

Figure 6: Exact solution  $u(0, x) = \sin \pi x$  and numerical solutions for  $\delta\% \in \{5\%, 15\%, 20\%\}$ . The final time  $t_f = 0.25$ ,  $t_0 = 10^{-3}$ ,  $m = 30$  and  $M = 30$ .

Table 1: Maximum error  $\|u(0, \cdot) - U\|_{L^\infty(\Omega)}$  with  $t_0 = 10^{-3}$ ,  $m = 30^2$ ,  $M = 10^2$ .

Noise	$t_f = 0.1$	$t_f = 0.5$	$t_f = 1$	$t_f = 1.5$	$t_f = 2.5$	$t_f = 3$
0%	7.5994e-007	4.8941e-007	4.9085e-007	4.9195e-007	4.6232e-006	8.6056e-003
1%	4.7273e-002	1.1895e-003	1.1810e-003	1.1805e-003	1.2448e-003	3.9789e-003
5%	8.5255e-002	5.8740e-003	5.9071e-003	5.9024e-003	5.6362e-003	5.7660e-003
15%	6.9104e-002	1.7640e-002	1.7722e-002	1.7713e-002	1.6776e-002	1.1838e-002
20%	6.8063e-002	2.3532e-002	2.3629e-002	2.3619e-002	2.2427e-002	1.4842e-002

### 6.3 Two-dimensional case

We consider the following two-dimensional case where  $\Omega = [0, 1] \times [0, 1]$ . We recover the initial distribution  $u(0, x, y) = \sin \pi x \sin \pi y$  of the exact solution

$$u(t, x, y) = \sin \pi x \sin \pi y \exp(-\pi^2 t).$$

for heat equation (8) from the data at  $t_f = 0.5$  so that we compare our result with the one obtained by [18]. On the basis of the investigation for 1D case in the previous section, we only treat the case of  $t_0 = 10^{-3}$ ,  $m = 30^2$ . The points  $X_m = \{x_1, \dots, x_m\}$  are equally distributed in  $\Omega$ , i.e.,  $X_m = \{(\frac{i}{m+1}, \frac{j}{m+1}) \mid i, j = 1, \dots, m\}$ . Since the numerical results are not sensitive to the number of measurement points, we fix  $M = 10^2$ . The measurement points  $Z_M$  are equally distributed in the domain as well. We give numerical results for noise-free case with various final observation time  $t_f = \{0.1, 0.5, 1, 1.5, 2.5, 3\}$  and noise level  $\delta\% \in \{0\%, 1\%, 5\%, 15\%, 20\%\}$ . As 1D case, we select  $\alpha$  as  $\alpha = 10^{-5} \frac{\max(A^* A)}{\max(B)}$  for the noise-free case, and determine  $\alpha$  by using L-curve method for the noisy data case. Table 1 shows the maximum error of  $U$  and Table 2 shows the relative error of  $U$ , where  $U$  denotes the reconstructed numerical solution. Even in the case of  $t_f = 3$  where the order of the exact solution  $u(t_f, \cdot)$  is about  $O(10^{-26})$ , the numerical results for all noisy cases are satisfactory.

Table 2: Relative error  $\frac{\|u(0, \cdot) - U\|_{L^2(\Omega)}}{\|u(0, \cdot)\|_{L^2(\Omega)}}$  with  $t_0 = 10^{-3}$ ,  $m = 30^2$ ,  $M = 10^2$ .

Noise	$t_f = 0.1$	$t_f = 0.5$	$t_f = 1$	$t_f = 1.5$	$t_f = 2.5$	$t_f = 3$
0%	8.5862e-007	4.9031e-007	4.9031e-007	4.9031e-007	1.2676e-006	3.4250e-003
1%	3.4029e-002	1.1796e-003	1.1813e-003	1.1809e-003	1.1407e-003	1.8338e-003
5%	7.4784e-002	5.8729e-003	5.9085e-003	5.9040e-003	5.6122e-003	4.0537e-003
15%	6.3677e-002	1.7641e-002	1.7726e-002	1.7718e-002	1.6777e-002	1.0491e-002
20%	6.2946e-002	2.3534e-002	2.3635e-002	2.3625e-002	2.2434e-002	1.3572e-002

## 7 Conclusion

In this paper we apply the discretized Tikhonov regularization by reproducing kernel Hilbert space to reconstruct the solution of the backward heat conduction problem. The implementation of the method is simple and easy. Numerical examples verify that the proposed method is efficient and accurate.

## References

- [1] N. Aronszajn, Theory of reproducing kernels, *Trans. Amer. Math. Soc.* 68 (1950) 337–404.
- [2] A. L. Bukhgeim, Introduction to the Theory of Inverse Problems, V.S.P. Intl Science, 1999.
- [3] A. Carasso, Error bounds in the final value problem for the heat equation, *SIAM J. Math. Anal.* 7 (1976) 195–199.
- [4] J.-R. Chang, C.-S. Liu, C.-W. Chang, A new shooting method for quasi-boundary regularization of backward heat conduction problems, *Int. J. Heat Mass Transfer* 50 (2007) 2325–2332.
- [5] L. Chiwiacowsky, H. de Campos Velho, Different approaches for the solution of a backward heat conduction problem, *Inverse Probl. Eng.* 11 (2003) 471–494.
- [6] E. B. Davies, Heat kernels and spectral theory, vol. 92 of Cambridge Tracts in Mathematics, Cambridge University Press, Cambridge, 1990.
- [7] C.-L. Fu, X.-T. Xiong, Z. Qian, Fourier regularization for a backward heat equation, *J. Math. Anal. Appl.* 331 (2007) 472–480.
- [8] X. Gao, X. T. Xiong, Y. Nie, C. L. Fu, Fourier regularization method for solving a backward heat conduction problem, *J. Lanzhou Univ. Nat. Sci.* 42 (2006) 119–120.
- [9] C. W. Groetsch, The theory of Tikhonov regularization for Fredholm equations of the first kind, Pitman, Boston, MA, 1984.
- [10] H. Han, D. Ingham, Y. Yuan, The boundary element method for the solution of the backward heat conduction equation, *J. Comput. Phys.* 116 (1995) 292–299.
- [11] P. C. Hansen, D. P. O’Leary, The use of the  $L$ -curve in the regularization of discrete ill-posed problems, *SIAM J. Sci. Comput.* 14 (1993) 1487–1503.
- [12] K. Iijima, K. Onishi, Lattice-free finite difference method for numerical solution of inverse heat conduction problem, *Inverse Probl. Sci. Eng.* 15 (2007) 93–106.
- [13] S. Itô, Diffusion equations, vol. 114 of Translations of Mathematical Monographs, American Mathematical Society, Providence, RI, 1992.
- [14] S. Kirkup, M. Wadsworth, Solution of inverse diffusion problems by operator-splitting methods, *Appl. Math. Modelling* 26 (2002) 1003–1018.
- [15] R. Lattès, J.-L. Lions, The method of quasi-reversibility. Applications to partial differential equations, American Elsevier Publishing Co., Inc., New York, 1969.
- [16] T. Lin, R. Ewing, A direct numerical method for an inverse problem for the heat equation via hyperbolic perturbation, *Decision and Control, 1988., Proceedings of the 27th IEEE Conference on* (1988) 240–244 vol.1.

- [17] C.-S. Liu, Group preserving scheme for backward heat conduction problems, *Int. J. Heat Mass Transfer* 47 (2004) 2567–2576.
- [18] J. Liu, Numerical solution of forward and backward problem for 2-D heat conduction equation, *J. Comput. Appl. Math.* 145 (2002) 459–482.
- [19] T. Matsuura, S. Saitoh, D. D. Trong, Approximate and analytical inversion formulas in heat conduction on multidimensional spaces, *J. Inverse Ill-Posed Probl.* 13 (2005), 479–493.
- [20] N. Mera, L. Elliott, D. DB Ingham, An inversion method with decreasing regularization for the backward heat conduction problem, *Numerical Heat Transfer, Part B* 42 (2002) 215–230.
- [21] N. Mera, L. Elliott, D. Ingham, D. Lesnic, An iterative boundary element method for solving the one dimensional backward heat conduction problem, *Int. J. Heat Mass Transfer* 44 (2001) 1937–1946.
- [22] N. S. Mera, The method of fundamental solutions for the backward heat conduction problem, *Inverse Probl. Sci. Eng.* 13 (2005) 65–78.
- [23] W. Muniz, F. Ramos, H. de Campos Velho, Entropy- and Tikhonov-based regularization techniques applied to the backwards heat equation, *Comput. Math. Appl.* 40 (2000) 1071–1084.
- [24] W. B. Muniz, H. F. de Campos Velho, F. M. Ramos, A comparison of some inverse methods for estimating the initial condition of the heat equation, *J. Comput. Appl. Math.* 103 (1999) 145–163.
- [25] L. E. Payne, *Improperly posed problems in partial differential equations*, Society for Industrial and Applied Mathematics, Philadelphia, Pa., 1975.
- [26] Z. Qian, C.-L. Fu, R. Shi, A modified method for a backward heat conduction problem, *Appl. Math. Comput.* 185 (2007) 564–573.
- [27] S. Saitoh, *Theory of reproducing kernels and its applications*, vol. 189 of Pitman Research Notes in Mathematics Series, Longman Scientific & Technical, UK, 1988.
- [28] R. Schaback, Solving the Laplace equation by meshless collocation using harmonic kernels, *Adv. in Comp. Math* 28 (2008) 283–299.
- [29] S.-Y. Shen, A numerical study of inverse heat conduction problems, *Comput. Math. Appl.* 38 (1999) 173–188.
- [30] A. Shidfar, A. Zakeri, A numerical technique for backward inverse heat conduction problems in one-dimensional space, *Appl. Math. Comput.* 171 (2005) 1016–1024.
- [31] T. Takeuchi, M. Yamamoto, Tikhonov regularization by a reproducing kernel Hilbert space for the Cauchy problem for an elliptic equation, *SIAM J. Sci. Comput.* 31 (2008) 112–142.
- [32] A. N. Tikhonov, V. Y. Arsenin, *Solutions of ill-posed problems*, John Wiley & Sons, New York, 1977.

- [33] A. N. Tikhonov, A. V. Goncharsky, V. V. Stepanov, A. G. Yagola, Numerical methods for the solution of ill-posed problems, Kluwer Academic Publishers Group, Dordrecht, 1995.
- [34] H. Wendland, Scattered Data Approximation, Cambridge Monographs on Applied and Computational Mathematics, Cambridge University Press, Cambridge, 2005.
- [35] X.-T. Xiong, C.-L. Fu, Z. Qian, Two numerical methods for solving a backward heat conduction problem, Appl. Math. Comput. 179 (2006) 370–377.
- [36] M. Yamamoto, J. Zou, Simultaneous reconstruction of the initial temperature and heat radiative coefficient, Inverse Problems 17 (2001) 1181–1202.

UTMS

- 2008–19 Oleg Yu. Imanouilov, Gunther Uhlmann, and Masahiro Yamamoto: *Partial data for the Calderón problem in two dimensions.*
- 2008–20 Xuefeng Liu and Fumio Kikuchi: *Analysis and estimation of error constants for  $P_0$  and  $P_1$  interpolations over triangular finite elements.*
- 2008–21 Fumio Kikuchi, Keizo Ishii and Issei Oikawa: *Discontinuous Galerkin FEM of Hybrid displacement type – Development of polygonal elements –.*
- 2008–22 Toshiyuki Kobayashi and Gen Mano: *The Schrödinger model for the minimal representation of the indefinite orthogonal group  $O(p, q)$ .*
- 2008–23 Kensaku Gomi and Yasuaki Mizumura: *A Completeness Theorem for the Logical System MPCL Designed for Mathematical Psychology.*
- 2008–24 Kensaku Gomi: *Theory of Completeness for Logical Spaces.*
- 2008–25 Oleg Yu. Imanuvilov, Gunther Uhlmann, and Masahiro Yamamoto: *Uniqueness by Dirichlet-to-Neumann map on an arbitrary part of boundary in two dimensions.*
- 2008–26 Takashi Tsuboi: *On the uniform simplicity of diffeomorphism groups.*
- 2008–27 A. Benabdallah, M. Cristofol, P. Gaitan and M. Yamamoto: *Inverse problem for a parabolic system with two components by measurements of one component.*
- 2008–28 Kensaku Gomi: *Foundations of Algebraic Logic.*
- 2008–29 Toshio Oshima: *Classification of Fuchsian systems and their connection problem.*
- 2008–30 Y. C. Hon and Tomoya Takeuchi: *Discretized Tikhonov regularization by a reproducing kernel Hilbert space for backward heat conduction problem.*

The Graduate School of Mathematical Sciences was established in the University of Tokyo in April, 1992. Formerly there were two departments of mathematics in the University of Tokyo: one in the Faculty of Science and the other in the College of Arts and Sciences. All faculty members of these two departments have moved to the new graduate school, as well as several members of the Department of Pure and Applied Sciences in the College of Arts and Sciences. In January, 1993, the preprint series of the former two departments of mathematics were unified as the Preprint Series of the Graduate School of Mathematical Sciences, The University of Tokyo. For the information about the preprint series, please write to the preprint series office.

ADDRESS:

Graduate School of Mathematical Sciences, The University of Tokyo  
3–8–1 Komaba Meguro-ku, Tokyo 153-8914, JAPAN  
TEL +81-3-5465-7001 FAX +81-3-5465-7012